

Tissue Metabolomics of Hepatocellular Carcinoma: Tumor Energy Metabolism and the Role of Transcriptomic Classification

Diren Beyoğlu,¹ Sandrine Imbeaud,^{2,3} Olivier Maurhofer,¹ Paulette Bioulac-Sage,^{4,5} Jessica Zucman-Rossi,^{2,3} Jean-François Dufour,¹ and Jeffrey R. Idle¹

Hepatocellular carcinoma (HCC) is one of the commonest causes of death from cancer. A plethora of metabolomic investigations of HCC have yielded molecules in biofluids that are both up- and down-regulated but no real consensus has emerged regarding exploitable biomarkers for early detection of HCC. We report here a different approach, a combined transcriptomics and metabolomics study of energy metabolism in HCC. A panel of 31 pairs of HCC tumors and corresponding nontumor liver tissues from the same patients was investigated by gas chromatography-mass spectrometry (GCMS)-based metabolomics. HCC was characterized by ~2-fold depletion of glucose, glycerol 3- and 2-phosphate, malate, alanine, *myo*-inositol, and linoleic acid. Data are consistent with a metabolic remodeling involving a 4-fold increase in glycolysis over mitochondrial oxidative phosphorylation. A second panel of 59 HCC that had been typed by transcriptomics and classified in G1 to G6 subgroups was also subjected to GCMS tissue metabolomics. No differences in glucose, lactate, alanine, glycerol 3-phosphate, malate, *myo*-inositol, or stearic acid tissue concentrations were found, suggesting that the Wnt/ β -catenin pathway activated by *CTNNB1* mutation in subgroups G5 and G6 did not exhibit specific metabolic remodeling. However, subgroup G1 had markedly reduced tissue concentrations of 1-stearoylglycerol, 1-palmitoylglycerol, and palmitic acid, suggesting that the high serum α -fetoprotein phenotype of G1, associated with the known overexpression of lipid catabolic enzymes, could be detected through metabolomics as increased lipid catabolism. **Conclusion:** Tissue metabolomics yielded precise biochemical information regarding HCC tumor metabolic remodeling from mitochondrial oxidation to aerobic glycolysis and the impact of molecular subtypes on this process. (HEPATOLOGY 2013;58:229-238)

Hepatocellular carcinoma (HCC) is the third leading cause of death from cancer worldwide and the ninth leading cause of cancer deaths in the United States.¹ An estimated 78% of global HCC cases have been attributed to chronic hepatitis B virus (HBV) and chronic hepatitis C virus (HCV) infection.² Therefore, HCC is closely associated with the underlying chronic liver diseases of hepatitis and

cirrhosis. The only chance of long-term disease-free survival for such patients is considered to depend on early diagnosis of HCC in asymptomatic patients.³ Methodologies for this involving ultrasound,⁴ micro-RNA panels,⁵ and various proteins, most notably α -fetoprotein (AFP),⁶ but screening using AFP and other circulating tumor markers suffers from a lack of both sensitivity and specificity.⁶ As has been recently

Abbreviations: AFP, α -fetoprotein; BHT, butylated hydroxytoluene; DEN, diethylnitrosamine; GCMS, gas chromatography-mass spectrometry; HBV, hepatitis B virus; HCC, hepatocellular carcinoma; LPC, lysophosphocholine; PCA, principal components analysis; PET, positron emission tomography; PI3, inositol triphosphate; PLS-DA, partial least squares projection to latent structures-discriminant analysis; OPLS-DA, orthogonal PLS-DA; Q2, predicted residual sum of squares; R2, sum of squares explained by the model.

From the ¹Hepatology Research Group, Department of Clinical Research, University of Bern, Switzerland; ²Inserm, UMR-674, Génomique fonctionnelle des tumeurs solides, IUH, Paris, France; ³Université Paris Descartes, Labex Immuno-oncology, Sorbonne Paris Cité, Faculté de Médecine, Assistance Publique-Hôpitaux de Paris, France; ⁴Inserm, UMR-1053; Université Victor Segalen Bordeaux 2, Bordeaux, France; ⁵CHU de Bordeaux, Pellegrin Hospital, Department of Pathology, Bordeaux, France.

Received December 4, 2012; accepted February 19, 2013.

Supported in part by National Institutes of Health/National Institute of Allergy and Infectious Diseases grant U19 AI067773-07/08 (to J.R.I.); Bernerische und Schweizerische Krebsliga, Sasella Foundation, and the Hassan Badawi Foundation Against Liver Cancer (to J.R.I., J.F.D.); this work was also the PAIR-CHC project NoFLIC (funded by INCa and Association pour la recherche contre le Cancer, ARC), the Réseau national CRB Foie and BioIntelligence (OSEO).

stated, there is an urgent need to identify new biomarkers without such limitations.⁶ The emerging omics technologies, such as metabolomics, provide an obvious starting point for such a search.

Metabolomics is the global and unbiased survey of the complement of small molecules (<1 kDa) in a biofluid, tissue, organ, or organism.⁷ Transcriptomics has been the principal omics tool employed to investigate HCC. As commented elsewhere, these gene expression studies conducted on HCC patient material and mouse models make virtually no mention of the genes involved in the metabolism of small cellular metabolites.⁸ However, there have been at least 12 published metabolomic studies addressing various aspects of HCC in patients. Nine of these have employed metabolomic analysis on either serum,⁹⁻¹⁶ plasma,⁸ or urine.^{9,17,18} Three further studies have been conducted in laboratory rodents, one in nude mice with xenografted HCC¹⁹ and two in rats with HCC and pulmonary metastases induced by administration of diethylnitrosamine (DEN).^{20,21} These rat studies were the only two investigations that determined metabolite profiles in HCC and control liver tissues. A single human study has been reported where HCC tissue and uninvolved liver tissue was analyzed.²² The majority of the human studies were conducted in China and with HCC patients who were predominantly HBV-positive.^{9,12-17} The aforementioned human studies have sought to define metabolomic biomarkers for the early detection of HCC in cirrhosis patients and have produced a plethora of molecules that are either up- or down-regulated in biofluids from HCC relative to healthy volunteers or cirrhosis patients. While these reports appear to show some general trends, mostly in bile salt and phospholipid serum profiles, the overall picture is still nebulous and a universal set of biomarkers with high specificity for HCC and high sensitivity for small tumors remains elusive.

We have chosen to adopt a different approach in the metabolomic investigation of HCC. There have been successful efforts to subclassify HCC tumor material using DNA microarrays. In one such global transcriptomic analysis,²³ six robust subgroups of HCC (G1-G6) were associated with genetic and epigenetic

alterations accumulated during tumor progression and reflected the diversity of HCC. Subsequently, this HCC tissue resource has been expanded and each sample characterized for genetic mutations and deletions relevant to HCC pathogenesis, including strong suggestions for a role of WNT/ β -catenin signaling in the management of oxidative stress and in the RAS/MAPK signaling pathway.²⁴ Here, we describe a gas chromatography-mass spectrometry (GCMS)-based metabolomic study of HCC tissue classified as G1 through G6, together with nontumorous tissue from the same livers. This is the first study to combine transcriptomics with metabolomics in the investigation of HCC. We report not only highly significant tumor depletion of glucose relative to uninvolved liver, but also a highly significant reduction of glycerol 3-phosphate, glycerol 2-phosphate, malate, alanine, and *myo*-inositol. The metabolomic analysis did not establish evidence for an association between increased glycolysis and any particular HCC subgroup. However, there was clear evidence of up-regulated fatty acid catabolism in G1 and, to a lesser extent, G3 HCC subgroups.

Materials and Methods

Tissue Samples. For the metabolomic comparison of HCC tumor tissue and uninvolved tissue from the same livers, a set of 31 pairs of tumor (T1) and uninvolved (N1) tissues were transported for analysis in Bern from Paris on dry ice. The samples were collected from Bordeaux surgical departments between 1999 to 2007 and had been stored at -80°C . A clinical description of these tissues has been reported.²³⁻²⁵ All 62 samples were analyzed as a single batch. For the metabolomic comparison of the different HCC subgroups G1 to G6,²³ 59 tumor samples, including the 31 T1 samples plus 28 additional tumor samples (T2) were analyzed, comprising five G1, seven G2, 11 G3, 18 G4, 11 G5, and seven G6 tumors. The essential characteristics of tumor groups G1 to G6 are given in Table 1.

Extraction of Tissue Samples for GCMS. All 62 samples for the T1 versus N1 study and 59 samples for the G1 to G6 study were analyzed as two single

Address reprint requests to: Professor Jeffrey R. Idle, Hepatology Research Group, Department of Clinical Research, University of Bern, Murtenstrasse 35, 3010 Bern, Switzerland. E-mail: jeff.idle@ikp.unibe.ch; fax: +41 31 941 03 76.

Copyright © 2013 by the American Association for the Study of Liver Diseases.

View this article online at wileyonlinelibrary.com.

DOI 10.1002/hep.26350

Potential conflict of interest: Nothing to report.

Additional Supporting Information may be found in the online version of this article.

Table 1. Essential Characteristics of HCC Transcriptomic Groups G1 to G6

Transcriptomic group	Characteristics
G1	Associated with HBV infection Low copy number of viral DNA <i>AXIN1</i> mutations Younger age High serum AFP Frequently of African origin <u>Overexpressed genes:</u> <i>MYH4, SOX9, IGF2, PEG3, PEG10, AFP, SGCE</i>
G2	Associated with HBV infection High copy number of viral DNA Frequent local and vascular invasion <i>TP53</i> and <i>AXIN1</i> mutations
G3	<i>TP53</i> mutations without HBV infection Chromosome losses at 17p, 5q, 21q, and 22q <i>CDKN2A</i> (p16 ^{ink4a} gene) promoter hypermethylation <u>Overexpressed genes:</u> <i>CDC6, MAD2L1, BUB1, TTK, SMC1L1, CCNA2, CCNE2, MCM2, MCM3, MCM6, ASK, KPNB1, RANBP5, XPO1, IPO7, NUP155, NUP107</i>
G4	Heterogeneous group of tumors that clustered with nontumorous livers 4/20 had <i>TCF1</i> (<i>HNF1A</i> gene) mutation and clustered with hepatocellular adenoma and well-differentiated HCC
G5	Activation of Wnt and β -catenin (70% <i>CTNNB1</i> mutations) <u>Overexpressed genes:</u> <i>GPR49, GLUL, PAP/HIP</i> (β -catenin target genes in the liver) <u>Underexpressed genes:</u> <i>ARHG-DIB, HLA-DPA1/B1, IFI16, IFI44, PTGER4, STAT1, CLECSF2</i>
G6	Activation of Wnt and β -catenin (100% <i>CTNNB1</i> mutations) with underexpression of cell adhesion proteins Putative β -catenin target gene expression > G5 Overexpression of β -catenin > G5 <u>Overexpressed genes:</u> <i>GPR49, GLUL, PAP/HIP, LEF1</i> <u>Underexpressed genes:</u> <i>CDH1</i> , highly correlated with downregulation of E-cadherin protein

Taken from published data.²³

batches on separate occasions. For preparation of GCMS, tissue samples were dissected while still frozen and a weighed amount (N1, 1.0-10.9 mg, mean \pm standard deviation [SD], 4.6 \pm 2.3 mg; T1, 1.0-10.1 mg, 4.6 \pm 2.1 mg; T2, 0.4-8.3 mg, 2.7 \pm 1.8 mg) was subjected to a modified Folch extraction²⁶ as follows: the frozen dissected tissues were homogenized in chloroform/methanol (2:1 v/v; 500 μ L, containing 0.01% butylated hydroxytoluene [BHT] as antioxidant and 200 μ M 4-chlorophenylacetic acid as internal standard) in 2-mL Eppendorf tubes by the addition of a stainless steel bead and agitation for 2 minutes at room temperature in a mixer mill, followed by dilution to 1,000 μ L with chloroform/methanol (2:1 v/v), and agitated for 20 minutes in an end-over-end shaker. Aqueous NaCl solution (0.9%; 500 μ L) was added,

the tubes inverted, then the supernatants transferred to 1.5-mL Eppendorf tubes, which were quickly vortexed and centrifuged at 2,000 rpm and 4°C for 20 minutes. Upper aqueous and lower organic layers were carefully separated by pipette. Both aqueous and organic fractions were blown to dryness under nitrogen and stored in screw-capped Eppendorf tubes at -80°C until analyzed by GCMS.

GCMS Analyses. For the analysis of the hydrophobic free and esterified fatty acids, frozen organic residues (chloroform extracts) were analyzed in triplicate by GCMS with three independent sample preparations using heptadecanoic acid as internal standard and acetyl chloride in methanol for methylation of free fatty acids and transmethylation of fatty acid esters, such as mono-, di-, and triglycerides, as described elsewhere.^{8,27} Samples were analyzed on a Supelcowax 10 capillary column (0.25 μ m film thickness; 30 m \times 0.25 mm i.d.; Sigma-Aldrich Chemie, Buchs, Switzerland) using an Agilent 6890N gas chromatograph fitted with an Agilent 7683B series automatic liquid sampler and an Agilent 5975B series mass selective detector from Agilent Technologies (Santa Clara, CA). For the analysis of hydrophilic metabolites in the tissues, frozen aqueous residues (saline extracts) were analyzed in triplicate by GCMS with three independent sample preparations using sequential methoxamine hydrochloride and BSTFA/TMCS derivatizations as described.²⁸ GCMS instrumentation was as above but with an Agilent HP-5MS capillary column (0.25 μ m film thickness; 60 m \times 0.25 mm i.d.). The source of authentic standards and reagents has been described in detail elsewhere.^{8,27,28} For the GCMS analysis of tissue extracts, chromatographic peaks were annotated first by comparison of their mass spectra with library spectra (~575,000 spectra in the NIST/EPA/NIH Mass Spectral Library v. 2.0, National Institutes of Standards and Technology, Gaithersburg, MD) and subsequently with authentic standards. Relative concentrations for each annotated metabolite were determined from the peak area ratio to internal standard area (hydrophobic metabolite assay, heptadecanoic acid; hydrophilic metabolite assay, 4-chlorophenylacetic acid). Triplicates were averaged after removal of any rogue values (~5% of cases) and means exported for multivariate data analysis and univariate statistics as described.²⁹

Multivariate Data Analysis. All data were exported from Excel, Pareto-scaled, and further analyzed by principal components analysis (PCA), partial least squares projection to latent structures-discriminant analysis (PLS-DA), and orthogonal PLS-DA (OPLS-DA) using SIMCA 13.0 (Umetrics AB, Umeå, Sweden).

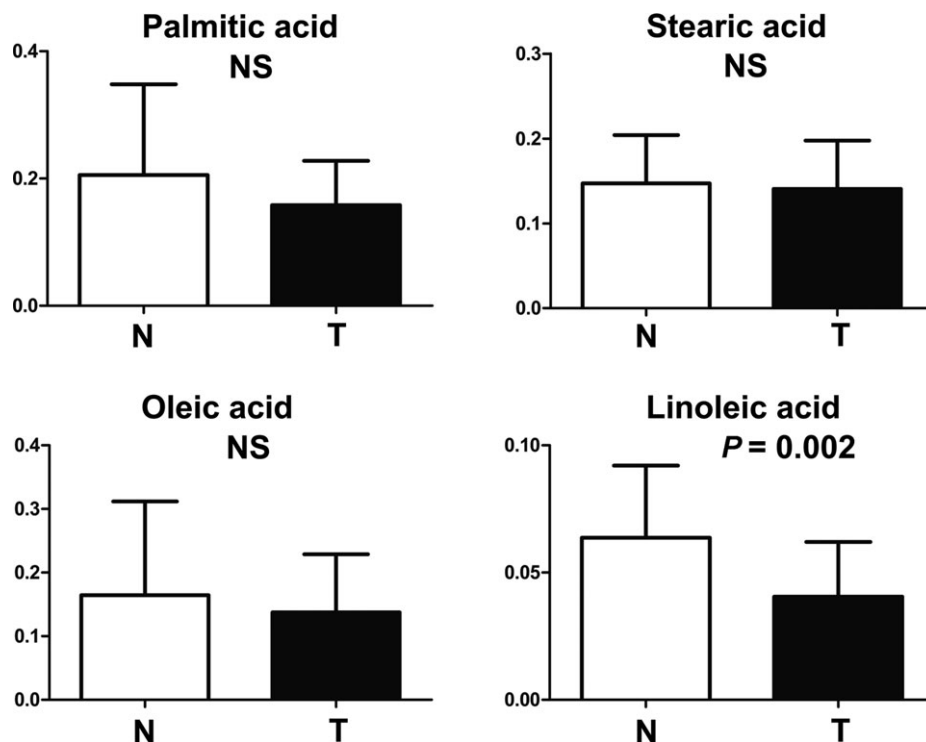


Fig. 1. Total fatty acid (free and esterified) content of 31 paired tumor (T) and uninvolved (N) tissues. Ordinates are relative concentrations (peak area/internal standard peak area/mg tissue). NS, not statistically significant.

Univariate Statistics. Data were exported from Excel into GraphPad Prism (v. 5, GraphPad Software, La Jolla, CA) and first inspected visually. For comparison of results for paired uninvolved (N1) and tumor (T1) tissues, Wilcoxon matched pairs test was used. For comparison of results between the T1+T2 groups G1 to G6, the Kruskal-Wallis test with Dunn's correction for multiple comparisons was used. For comparisons of lipid tissue levels between N1 and T1 tissues, an unpaired Student's *t* test was used. For comparison of lipid tissue levels between G1, G2, G4, and G6, the Kruskal-Wallis test with Dunn's correction for multiple comparisons was used. For comparison of lipid tissue levels between G1 and G2-G6 combined, Mann-Whitney *U* test was used.

Results

Only nine fatty acids (free and esterified) were identified and thus quantitated in HCC tumors and paired uninvolved liver samples by GCMS analysis of fatty acid methyl esters. This is somewhat less than the 13 fatty acids detected in HCC and control plasma.⁸ Only four fatty acids were present in all 62 T1 and N1 tissue samples, namely, palmitic acid, stearic acid, oleic acid, and linoleic acid. Accordingly, multivariate data analysis was not required to evaluate these data. Figure 1 shows that only linoleic acid was statistically significantly different ($P = 0.002$) and diminished in

T1 compared to N1. This observation suggests that uninvolved parenchyma in a liver harboring HCC may have a similar rate of mitochondrial β -oxidation as the tumor itself. Moreover, since linoleic acid is the obligate starting point for *de novo* synthesis of arachidonic acid by desaturation and chain elongation,³⁰ HCC may engage in enhanced arachidonic acid synthesis. It is well established that cyclooxygenase 2 is overexpressed in HCC leading to increased prostaglandin E2 signaling.³¹

A total of 44 peaks corresponding to 43 hydrophilic metabolites in the saline extracts of T1 and N1 were annotated and their mean relative concentrations (peak area/internal standard peak area/mg tissue) for each tissue sample analyzed by PLS-DA which gave a reasonable separation between T1 and N1 samples in the scores plot (Fig. 2A). PLS-DA model validation was performed using data permutation to degrade the fraction of the sum of squares explained by the model (R^2) and predicted residual sum of squares (Q^2) values. After 50 permutations R^2 and Q^2 were degraded to 0.2 and -0.2 , respectively (Fig. 2B), demonstrating that the data were not overfitted in the PLS-DA model. To discern which metabolites were most responsible for the separation between T1 and N1 scores (Fig. 2A), OPLS-DA analysis was performed and the findings expressed in a loadings S-plot (Fig. 2C). The six metabolites with the greatest correlation to the model were further investigated using univariate

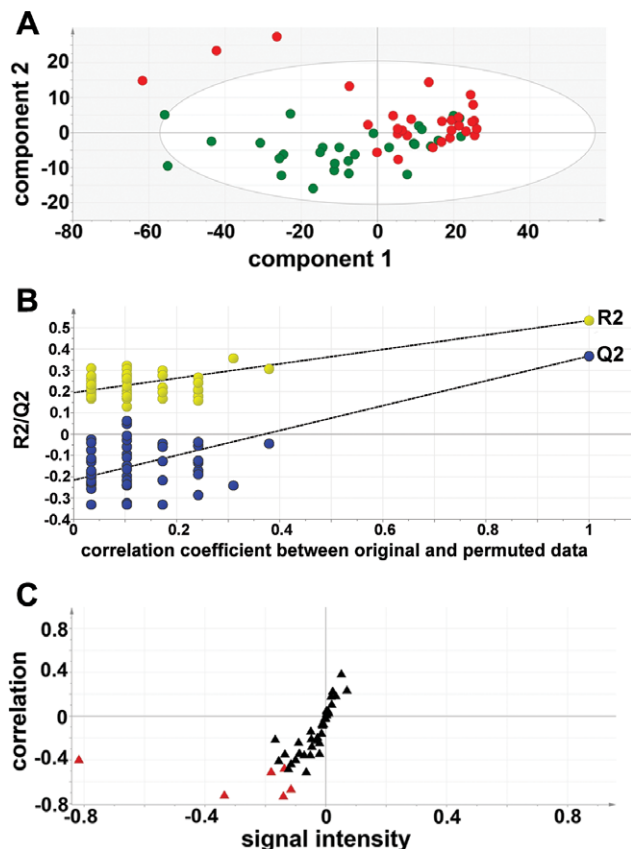


Fig. 2. GCMS tissue metabolomics of 31 paired HCC tumors and uninvolved liver. (A) PLS-DA scores plot showing almost complete separation of tumors (red) and uninvolved liver tissues (green). (B) Validation of the PLS-DA model by 50 permutations of the data showing degradation of R2 to below 0.3 and Q2 to below 0. (C) OPLS-DA loadings S-plot showing down-regulated metabolites (red) in tumor tissue that were significantly correlated with the OPLS-DA model. These metabolites comprised glucose, glycerol 3-phosphate, glycerol 2-phosphate, malate, alanine, and *myo*-inositol.

statistics. T1 levels of glucose, glycerol 3-phosphate, glycerol 2-phosphate, malate, alanine, and *myo*-inositol were all statistically significantly depressed below their paired N1 tissue levels (Fig. 3). Others²² have reported lower glucose in HCC tissue and this would be expected if the tumors operated aerobic glycolysis (Warburg effect).³² However, the down-regulation of glycerol 3- and 2-phosphate, malate, alanine, and *myo*-inositol is a novel observation. Together with lactate, alanine is a product of glycolysis when pyruvate is not directed into the citric acid cycle in mitochondria.³³ Malate transports reducing equivalents into mitochondria from glycolysis through the malate-aspartate shuttle³⁴ and glycerol 3-phosphate plays a similar secondary role in the glycerol 3-phosphate shuttle.³⁴ The depression of HCC tissue concentrations of glucose, alanine, malate, and glycerol 3-phosphate is suggestive of a high glycolytic conversion of glucose to pyruvate in cytosol followed by conversion to acetyl-CoA and

entry into the mitochondrial citric acid cycle, with little conversion of pyruvate to lactate or alanine.

GCMS analysis of 62 HCC samples that had been categorized into G1 to G6 subtypes was undertaken. Only hydrophilic metabolites were determined and metabolite identities and mean relative concentrations were determined and treated by multivariate data analysis. Three major outliers were detected in the PCA scores plot for all data (not shown) and these three samples were removed and the data reanalyzed using OPLS-DA. Pairwise analysis of all 15 possible combinations of G1 to G6 was made, and the loadings S-plots are shown in Fig. 4 for the pairs G1-G2, G1-G4, G1-G5, G1-G6, G3-G2, G3-G4, G3-G5, and G3-G6. These analyses showed that the monoacylglycerols 1-palmitoylglycerol and 1-stearoylglycerol were depressed in G1 and G3 HCC types relative to the other tumor classes. A more detailed Kruskal-Wallis analysis with Dunn's correction for multiple comparisons was undertaken on the six HCC classes. Figure 5 shows that there were no statistically significant differences between the tumor classes for lactate, glucose, glycerol 3-phosphate, malate, alanine, and *myo*-inositol. This suggests that glycolysis operates equally in each tumor type, despite G5 and G6 possessing elevated Wnt signaling and β -catenin activation.^{23,24} However, the aforementioned monoacylglycerols, together with their corresponding fatty acids, were virtually extinguished in G1 and G3, with statistically significant depression of both monoacylglycerols and palmitic acid in G1 relative to G4, and of 1-palmitoylglycerol in G1 relative to G2. Differences for stearic acid and for any molecule tested in G3 did not reach statistical significance. These same lipids were then compared for G1 versus G2 to G6 combined (Fig. 6). The findings support the view that the catabolism of palmitic acid, stearic acid, and their monoacylglycerol precursors is enhanced in HCC tumor type G1.

Discussion

GCMS-based metabolomic analysis of HCC tumor and uninvolved liver from 31 patients showed that tumor tissue had down-regulated levels of glucose, glycerol 3- and 2-phosphate, malate, alanine, *myo*-inositol, and linoleic acid. Additionally, HCC tumor tissue from transcriptomic groups G1 to G6 possessed similar levels of lactate, glucose, glycerol 3-phosphate, malate, alanine, *myo*-inositol, and stearic acid. However, HCC tumors typed as G1 had lower levels of 1-stearoylglycerol, 1-palmitoylglycerol, and palmitic acid than HCC tumors typed as G2 or G4, and lower

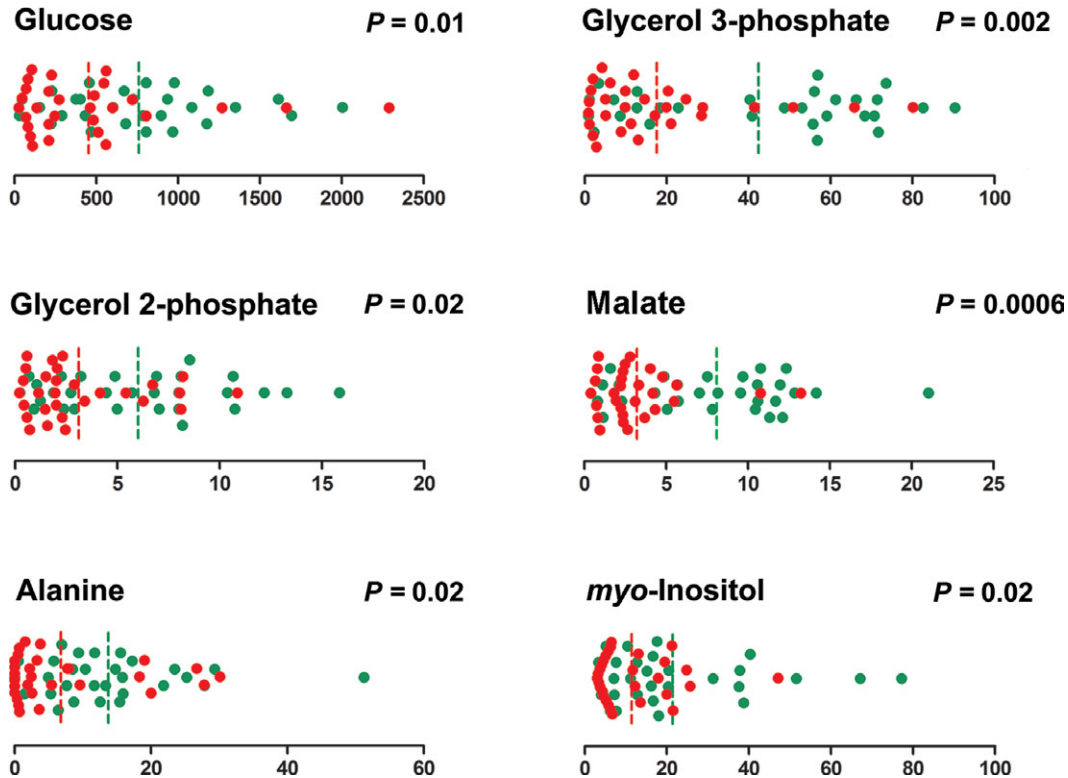


Fig. 3. Univariate statistical analysis of six metabolites identified as down-regulated in HCC tumor tissues by OPLS-DA analysis. Abscissae are relative concentrations (peak area/internal standard peak area/mg tissue). Red and green symbols represent tumor and unaffected tissue samples, respectively. Red and green dotted lines represent median values for tumor and unaffected tissue samples, respectively. Data were analyzed using Wilcoxon matched pairs test.

levels than all other transcriptomic tumor types combined.

High consumption of glucose by tumors with conversion through pyruvate to lactate and alanine,³³ a process known as aerobic glycolysis or the Warburg effect,³² is a well-studied phenomenon, including in HCC.³³ The increase in glycolysis, with an ~10-fold increase in conversion of glucose to lactic acid, occurs at the expense of mitochondrial citric acid cycle usage and oxidative phosphorylation.³⁵⁻³⁷ Many factors are involved in regulating the switch from mitochondrial oxidation to glycolysis³⁵⁻³⁷ and the discrete intracellular glycolytic signal is still unknown. However, Wnt has been reported to suppress mitochondrial respiration and cytochrome C oxidase activity in cell lines, while up-regulating pyruvate carboxylase, thus inducing a glycolytic switch with increased glucose consumption and lactate production³⁸ through up-regulated lactate dehydrogenase.³⁹ Moreover, HCC appears to exhibit suppression of gluconeogenesis by Stat3-mediated activation of the microRNA miR-23a that targets glucose-6-phosphatase expression.⁴⁰ However, Wnt/ β -catenin signaling was only observed in HCC transcriptomic groups G5 and G6 (Table 1), with no evidence of acti-

vation of this pathway in groups G1 to G4.²³ Clearly, at least in this set of tumors, Wnt/ β -catenin signaling alone did not appear to regulate the metabolic remodeling of HCC from mitochondrial oxidative metabolism to glycolysis, as judged by tumor glucose, lactate, and alanine concentrations (Fig. 5). Furthermore, reducing equivalents required by mitochondria, as reflected by malate and glycerol 3-phosphate concentrations,³⁴ were also not different between groups G1 to G6 (Fig. 5). However, concentrations of these were ~50% in tumors than in paired uninvolved tissues, as they were also for glucose (Fig. 3). Furthermore, the concentrations of malate and glycerol 3-phosphate were also ~50% in tumors, and this probably reflects a 50% down-regulation of mitochondrial oxidative phosphorylation which requires these reducing equivalents. Taken together, these data suggest that the metabolic remodeling of HCC from mitochondrial oxidation to glycolysis was ~4-fold, less than that for many other types of tumor.³² Interestingly, in a rat model of HCC, tumor lactate and alanine production from pyruvate was increased 2- and 5-fold, respectively.³³ All these observations fall far short of the 100-fold increase in lactate production for Flexner-Jobling rat liver carcinoma

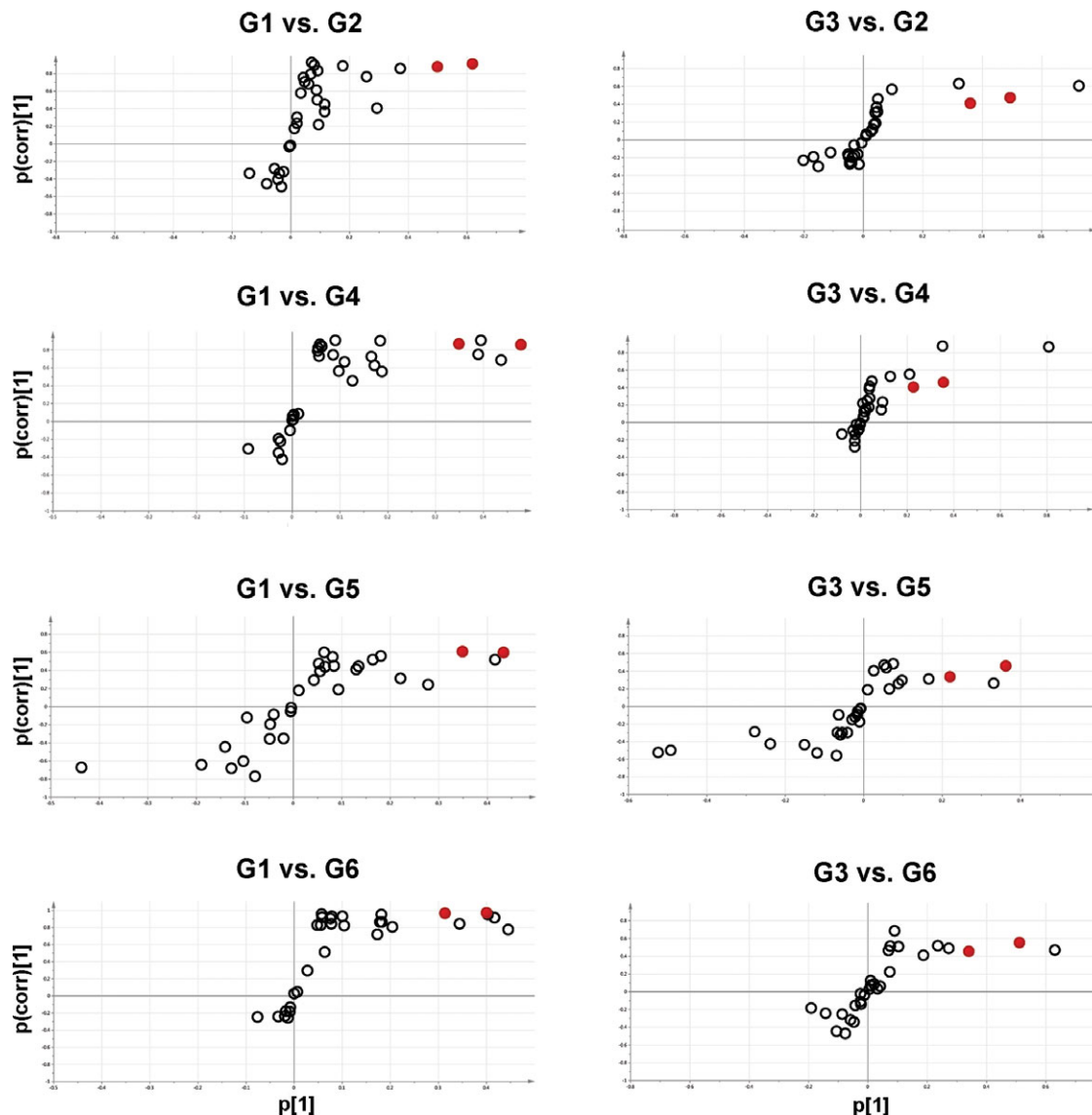


Fig. 4. OPLS-DA loadings S-plots for 59 HCC tissues typed as transcriptomic subgroups G1 to G6 and analyzed by GCMS. Of the 15 possible S-plots for G1 to G6, eight are shown for comparisons of G1 to G2, G4, G5, and G6, together with comparisons of G3 with G2, G4, G5, and G6. Abscissa units of $p[1]$ are proportional to concentration and ordinate units of $p(\text{corr})[1]$ are a measure of the correlation of any loading (metabolite) to the OPLS-DA model. Red symbols correspond to the monoacylglycerols 1-palmitoylglycerol and 1-stearoylglycerol, which were elevated in G2, G4, G5, and G6 relative to G1 with similar comparisons shown for G3.

reported by Warburg in 1924.³⁶ Furthermore, the use of 2-deoxy-2- ^{18}F fluoro-D-glucose positron emission tomography (PET) for the detection and monitoring of malignancies depends on a high uptake and concentration of glucose in tumor cells.³⁵ Given our metabolomics findings, it is hardly surprising that PET scanning is of limited value in the detection and target delineation of primary HCC,⁴¹ due to the meager metabolic differences between tumor and surrounding parenchyma. In fact, myofibroblasts in the tumor environment may contribute to HCC energy metabolism by releasing lactate that is taken up by the tumor in a process controlled by Hedgehog signaling.⁴²

Myo-inositol is a metabolic precursor of the inositol phosphate second messengers, phosphatidylinositol membrane lipids, and the phosphoinositide lipid signaling molecules.³⁴ The PI3K-AKT-mTOR pathway, which has been associated with induction of aerobic glycolysis and tumor metabolic remodeling,^{43,44} requires inositol triphosphate (PI3), and thus *myo*-inositol as a substrate. *Myo*-inositol is synthesized from glucose³⁴ and thus diminution of cellular glucose by enhanced metabolism is likely to impact cellular *myo*-inositol. In a study of breast cancer and normal breast tissues, *myo*-inositol and glucose were lower in the tumor samples.⁴⁵ The PI3K-AKT-mTOR pathway is perturbed in many

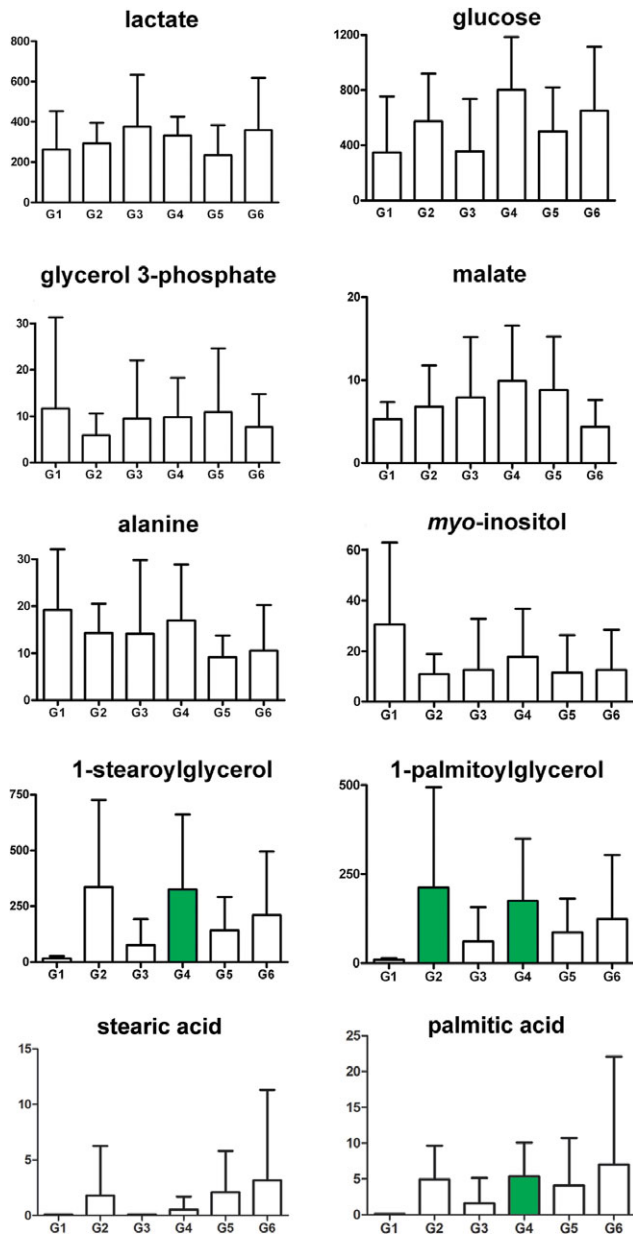


Fig. 5. Univariate statistical analysis for 10 metabolites in HCC tumor samples according to transcriptomic groups G1 to G6. Note no statistically significant differences in tissue lactate, glucose, glycerol 3-phosphate, malate, alanine, *myo*-inositol, and stearic acid across groups G1 to G6. Group G1 displayed significantly lower ($P < 0.05$) levels of 1-stearoylglycerol, 1-palmitoylglycerol, and palmitic acid than certain other groups (shown in green). Data were analyzed by Kruskal-Wallis with Dunn's correction for multiple comparisons.

cancers and it was recently reported that cell lines with mutated PI3K possess a highly glycolytic phenotype and withdrawal of glucose cannot be compensated by addition of alternative nutrients.⁴⁴ Whether or not our observation of an ~ 2 -fold attenuation of *myo*-inositol tumor concentrations (Fig. 3), with no difference between G1 to G6 (Fig. 5), is indicative of a change in PI3K-AKT-mTOR signaling is unknown at present.

Several changes in lipid levels between transcriptional groups G1 to G6 were observed in this study, most notably for 1-stearoylglycerol, 1-palmitoylglycerol, and palmitic acid, which were markedly depressed in the G1 subtype, statistically significantly lower than G4 (all three lipids) and G2 (1-palmitoylglycerol only; Fig. 5). Although palmitic, stearic, and oleic acid tumor levels were not found to be different from uninvolved liver, linoleic acid levels were approximately halved in tumor tissue (Fig. 1). These data are consistent with a similar rate of metabolism/synthesis of fatty acids in HCC tumor tissue and uninvolved liver, with the exception of linoleic acid. As stated above, this fatty acid is the starting point for the *de novo* synthesis of arachidonic acid by chain elongation and desaturation.³⁴ This finding may therefore reflect enhanced arachidonic acid synthesis in HCC tumor tissue. Regarding the attenuated lipids in G1, it should be recalled that many lysophosphocholines (LPCs) have been reported to be attenuated in the serum/plasma of HCC patients relative to controls.^{8,12} LPCs have also been reported to undergo enhanced biliary excretion in HCC.⁴⁶ 1-Acylglycerols are potentially synthesized by phospholipase action on LPCs and therefore the lower concentration of LPCs in HCC may generate less 1-acylglycerols. Moreover, HCC type G1 is associated with a high serum AFP concentration (Table 1). Liver cancer cell lines expressing varying amounts of AFP have been used to investigate genes whose expression significantly correlated with AFP expression. Microarray analysis revealed 11 genes involved in lipid catabolism that were associated with

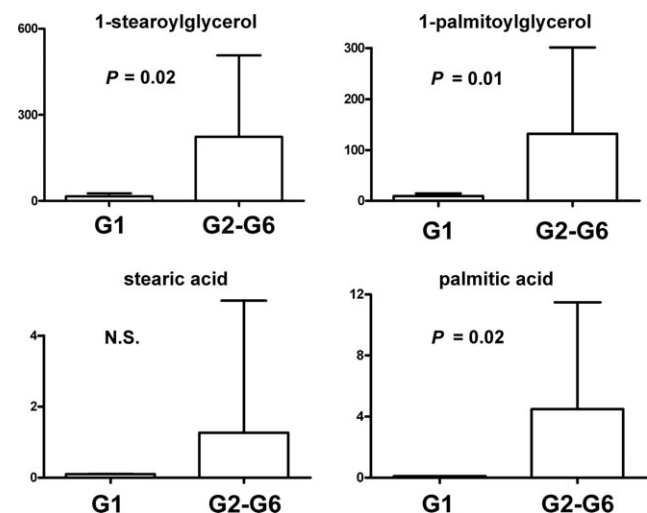


Fig. 6. Univariate statistical analysis for four metabolites in HCC tumor tissue transcriptomic group G1 versus all other groups G2-G6 combined. NS, not statistically significant. Data analyzed by two-tailed Mann-Whitney U test.

AFP expression.⁴⁷ The phenotype of G1 would appear to include increased lipid catabolism.

In summary, we report here that HCC has lower cellular levels of glucose and other metabolites involved in energy production. The data suggest a metabolic remodeling on the order of 4-fold towards glycolytic metabolism in tumor versus uninvolved liver tissue. Analysis of the tissue metabolome of transcriptomic subgroups G1 to G6 showed that the glycolysis molecules glucose, lactate, and alanine were equivalent between subgroups with different cell signaling networks, including G5 and G6 with activated Wnt/ β -catenin signaling. However, subgroup G1, which had the highest serum AFP concentrations, harbored diminished concentrations of certain saturated lipids, consistent with the up-regulation of lipid catabolism associated with elevated AFP expression. HCC would appear to be characterized by increased glycolysis, attenuated mitochondrial oxidation, and increased arachidonic acid synthesis. The transcriptomic subgroup G1 is associated with increased fatty acid catabolism. A study has just been reported in which monounsaturated palmitic acid was identified using a combined transcriptomic and metabolomic approach as a marker for HCC progression and poorer patient survival.⁴⁸

References

- Altekruse SF, McGlynn KA, Reichman ME. Hepatocellular carcinoma incidence, mortality, and survival trends in the United States from 1975 to 2005. *J Clin Oncol* 2009;27:1485-1491.
- Perz JE, Armstrong GL, Farrington LA, Hutin YJ, Bell BP. The contributions of hepatitis B virus and hepatitis C virus infections to cirrhosis and primary liver cancer worldwide. *J Hepatol* 2006;45:529-538.
- Forner A, Llovet JM, Bruix J. Hepatocellular carcinoma. *Lancet* 2012;379:1245-1255.
- Lencioni R. Surveillance and early diagnosis of hepatocellular carcinoma. *Dig Liver Dis* 2010;42(Suppl 3):S223-227.
- Chen CJ, Lee MH. Early diagnosis of hepatocellular carcinoma by multiple microRNAs: validity, efficacy, and cost-effectiveness. *J Clin Oncol* 2011;29:4745-4747.
- Forner A, Bruix J. Biomarkers for early diagnosis of hepatocellular carcinoma. *Lancet Oncol* 2012;13:750-751.
- Beyoglu D, Idle JR. Metabolomics and its potential in drug development. *Biochem Pharmacol* 2013;85:12-20.
- Patterson AD, Maurhofer O, Beyoglu D, Lanz C, Krausz KW, Pabst T, et al. Aberrant lipid metabolism in hepatocellular carcinoma revealed by plasma metabolomics and lipid profiling. *Cancer Res* 2011;71:6590-6600.
- Chen T, Xie G, Wang X, Fan J, Qiu Y, Zheng X, et al. Serum and urine metabolite profiling reveals potential biomarkers of human hepatocellular carcinoma. *Mol Cell Proteomics* 2011;10:M110 004945.
- Ressom HW, Xiao JF, Tuli L, Varghese RS, Zhou B, Tsai TH, et al. Utilization of metabolomics to identify serum biomarkers for hepatocellular carcinoma in patients with liver cirrhosis. *Anal Chim Acta* 2012;743:90-100.
- Xiao JF, Varghese RS, Zhou B, Nezami Ranjbar MR, Zhao Y, Tsai TH, et al. LC-MS based serum metabolomics for identification of hepatocellular carcinoma biomarkers in Egyptian cohort. *J Proteome Res* 2012;11:5914-5923.
- Zhou L, Wang Q, Yin P, Xing W, Wu Z, Chen S, et al. Serum metabolomics reveals the deregulation of fatty acids metabolism in hepatocellular carcinoma and chronic liver diseases. *Anal Bioanal Chem* 2012;403:203-213.
- Chen F, Xue J, Zhou L, Wu S, Chen Z. Identification of serum biomarkers of hepatocarcinoma through liquid chromatography/mass spectrometry-based metabolomic method. *Anal Bioanal Chem* 2011;401:1899-1904.
- Tan Y, Yin P, Tang L, Xing W, Huang Q, Cao D, et al. Metabolomics study of stepwise hepatocarcinogenesis from the model rats to patients: potential biomarkers effective for small hepatocellular carcinoma diagnosis. *Mol Cell Proteomics* 2012;11:M111 010694.
- Wang B, Chen D, Chen Y, Hu Z, Cao M, Xie Q, et al. Metabolomic profiles discriminate hepatocellular carcinoma from liver cirrhosis by ultraperformance liquid chromatography-mass spectrometry. *J Proteome Res* 2012;11:1217-1227.
- Yin P, Wan D, Zhao C, Chen J, Zhao X, Wang W, et al. A metabolomic study of hepatitis B-induced liver cirrhosis and hepatocellular carcinoma by using RP-LC and HILIC coupled with mass spectrometry. *Mol Biosyst* 2009;5:868-876.
- Wu H, Xue R, Dong L, Liu T, Deng C, Zeng H, et al. Metabolomic profiling of human urine in hepatocellular carcinoma patients using gas chromatography/mass spectrometry. *Anal Chim Acta* 2009;648:98-104.
- Ye G, Zhu B, Yao Z, Yin P, Lu X, Kong H, et al. Analysis of urinary metabolic signatures of early hepatocellular carcinoma recurrence after surgical removal using gas chromatography-mass spectrometry. *J Proteome Res* 2012;11:4361-4372.
- Li S, Liu H, Jin Y, Lin S, Cai Z, Jiang Y. Metabolomics study of alcohol-induced liver injury and hepatocellular carcinoma xenografts in mice. *J Chromatogr B Analyt Technol Biomed Life Sci* 2011;879:2369-2375.
- Li ZF, Wang J, Huang C, Zhang S, Yang J, Jiang A, et al. Gas chromatography/time-of-flight mass spectrometry-based metabolomics of hepatocarcinoma in rats with lung metastasis: elucidation of the metabolic characteristics of hepatocarcinoma at formation and metastasis. *Rapid Commun Mass Spectrom* 2010;24:2765-2775.
- Wang J, Zhang S, Li Z, Yang J, Huang C, Liang R, et al. (1)H-NMR-based metabolomics of tumor tissue for the metabolic characterization of rat hepatocellular carcinoma formation and metastasis. *Tumour Biol* 2011;32:223-231.
- Yang Y, Li C, Nie X, Feng X, Chen W, Yue Y, et al. Metabolomic studies of human hepatocellular carcinoma using high-resolution magic-angle spinning 1H NMR spectroscopy in conjunction with multivariate data analysis. *J Proteome Res* 2007;6:2605-2614.
- Boyault S, Rickman DS, de Reynies A, Balabaud C, Rebouissou S, Jeannot E, et al. Transcriptome classification of HCC is related to gene alterations and to new therapeutic targets. *HEPATOLOGY* 2007;45:42-52.
- Guichard C, Amaddeo G, Imbeaud S, Ladeiro Y, Pelletier L, Maad IB, et al. Integrated analysis of somatic mutations and focal copy-number changes identifies key genes and pathways in hepatocellular carcinoma. *Nat Genet* 2012;44:694-698.
- Laurent-Puig P, Legoix P, Bluteau O, Belghiti J, Franco D, Binot F, et al. Genetic alterations associated with hepatocellular carcinomas define distinct pathways of hepatocarcinogenesis. *Gastroenterology* 2001;120:1763-1773.
- Folch J, Lees M, Sloane Stanley GH. A simple method for the isolation and purification of total lipides from animal tissues. *J Biol Chem* 1957;226:497-509.
- Lanz C, Ledermann M, Slavik J, Idle JR. The production and composition of rat sebum is unaffected by 3 Gy gamma radiation. *Int J Radiat Biol* 2011;87:360-371.
- Lanz C, Patterson AD, Slavik J, Krausz KW, Ledermann M, Gonzalez FJ, et al. Radiated metabolomics. 3. Biomarker discovery in the urine of gamma-irradiated rats using a simplified metabolomics protocol of gas chromatography-mass spectrometry combined with random forests machine learning algorithm. *Radiat Res* 2009;172:198-212.

29. Fahrner R, Beyoglu D, Beldi G, Idle JR. Metabolomic markers for intestinal ischemia in a mouse model. *J Surg Res* 2012;178:879-887.
30. Brenner RR. The oxidative desaturation of unsaturated fatty acids in animals. *Mol Cell Biochem* 1974;3:41-52.
31. Wu T. Cyclooxygenase-2 in hepatocellular carcinoma. *Cancer Treat Rev* 2006;32:28-44.
32. Gatenby RA, Gillies RJ. Why do cancers have high aerobic glycolysis? *Nat Rev Cancer* 2004;4:891-899.
33. Darpolor MM, Yen YF, Chua MS, Xing L, Clarke-Katzenberg RH, Shi W, et al. In vivo MRSI of hyperpolarized [1-(13)C]pyruvate metabolism in rat hepatocellular carcinoma. *NMR Biomed* 2011;24:506-513.
34. Nelson DL, Cox MM. Lehninger. Principles of Biochemistry. 5th ed. New York: W.H. Freeman; 2008.
35. Cairns RA, Harris IS, Mak TW. Regulation of cancer cell metabolism. *Nat Rev Cancer* 2011;11:85-95.
36. Koppenol WH, Bounds PL, Dang CV. Otto Warburg's contributions to current concepts of cancer metabolism. *Nat Rev Cancer* 2011;11:325-337.
37. Vander Heiden MG, Cantley LC, Thompson CB. Understanding the Warburg effect: the metabolic requirements of cell proliferation. *Science* 2009;324:1029-1033.
38. Lee SY, Jeon HM, Ju MK, Kim CH, Yoon G, Han SI, et al. Wnt/Snail signaling regulates cytochrome C oxidase and glucose metabolism. *Cancer Res* 2012;72:3607-3617.
39. Chafey P, Finzi L, Boisgard R, Cauzac M, Clary G, Broussard C, et al. Proteomic analysis of beta-catenin activation in mouse liver by DIGE analysis identifies glucose metabolism as a new target of the Wnt pathway. *Proteomics* 2009;9:3889-3900.
40. Wang B, Hsu SH, Frankel W, Ghoshal K, Jacob ST. Stat3-mediated activation of microRNA-23a suppresses gluconeogenesis in hepatocellular carcinoma by down-regulating glucose-6-phosphatase and peroxisome proliferator-activated receptor gamma, coactivator 1 alpha. *HEPATOLOGY* 2012;56:186-197.
41. Lambrecht M, Haustermans K. Clinical evidence on PET-CT for radiation therapy planning in gastro-intestinal tumors. *Radiother Oncol* 2010;96:339-346.
42. Chan IS, Guy CD, Chen Y, Lu J, Swiderska M, Michelotti GA, et al. Paracrine Hedgehog signaling drives metabolic changes in hepatocellular carcinoma. *Cancer Res* 2012;72:6344-6350.
43. Finlay DK. Regulation of glucose metabolism in T cells: new insight into the role of phosphoinositide 3-kinases. *Front Immunol* 2012;3:247.
44. Foster R, Griffin S, Grooby S, Feltell R, Christopherson C, Chang M, et al. Multiple metabolic alterations exist in mutant pi3k cancers, but only glucose is essential as a nutrient source. *PLoS One* 2012;7:e45061.
45. Beckonert O, Monnerjahn J, Bonk U, Leibfritz D. Visualizing metabolic changes in breast-cancer tissue using 1H-NMR spectroscopy and self-organizing maps. *NMR Biomed* 2003;16:1-11.
46. Skill NJ, Scott RE, Wu J, Maluccio MA. Hepatocellular carcinoma associated lipid metabolism reprogramming. *J Surg Res* 2011;169:51-56.
47. Saito S, Ojima H, Ichikawa H, Hirohashi S, Kondo T. Molecular background of alpha-fetoprotein in liver cancer cells as revealed by global RNA expression analysis. *Cancer Sci* 2008;99:2402-2409.
48. Budhu A, Roessler S, Zhao X, Yu Z, Forgues M, Ji J, et al. Integrated metabolite and gene expression profiles identify lipid biomarkers associated with progression of hepatocellular carcinoma and patient outcomes. *Gastroenterology* 2013 [Epub ahead of print].